Research Article

Angiogenesis Related Remodeling and Reprogramming in Melanomas

Bhanu Iyengar

Pigment Cell Center, New Delhi, INDIA

Abstract

Introduction:

Melanomas show a wide variation in pigmentation. The present study evaluates the role of angiogenesis in reprogramming/remodeling of the tumor through tumor vascular interactions.

Methods:

Paraffin and frozen sections from melanomas in vertical growth phase, were subjected to routine, enzyme/Immunohistochemistry, and electron microscopy. Quantitation was done by morphometric analysis of cell/nuclear size and density and mitotic counts to compare pigmented, amelanotic areas and tumor-vascular-complexes[TVCs]. Progression and fate of TVCs was assessed in 3D constructs of angiogenic vessels.

Results:

Pigmented areas show marked variation in cell/nuclear size, nuclear content and abnormal mitosis. Cells in amelanotic areas are uniform, with near normal morphometric values and synchronization of mitosis. Vasculogenesis is evident in amelanotic zones.

Angiogenic tubes interact with tumor, forming 3D tumor-vascular-complexes [TVCs] with a central vessel and a perivascular mantle of cells, showing normal mitosis and regulated neural differentiation. Morphometric parameters and differentiation are graded proportionate to level of pigmentation.

Discussion:

TVCs grow into expansile nodules with peripheral pigmented layers which elicit further angiogenesis at the stromal margin. A cyclical process results in amelanotic nodules Angiogenesis from normal vasculature gives polarity and creates an embryonal microenvironment with reprogramming of pleomorphic pigmented to amelanotic near normal cells with embryonic characteristics. Clinically, the therapeutic strategies have to target both angiogenesis as well as the self propagating vascular networks.

Introduction

Melanocytes are derived from the multipotent neural crest cells[NC] during embryogenesis of the neural tube[1]. The NC cells arise from the neural fold which lies at the confluence of the neuroepithelium and the general epidermis. These cells differentiate into neuronal, epidermal as well as pigment cells. The melanocytes actively produce catecholamines as well as indoleamines[2–4]. Melanomas are highly malignant tumors arising from the melanocytes in the basal layer of the epidermis, uveal tract of the eyes, inner ear, mucous membrane, genital organs, anus and leptomeninges.

Human cutaneous melanomas show molecular plasticity and often express genes characteristic of neural cell lineages[5]. In vertical growth phase[VGP] melanomas there is a definite pattern of neural differentiation in relation to angiogenesis

on viewing the tumor vascular interaction as a three dimensional system[6].

Human cancers which persist in situ for months in a prevascular phase, require efficient vascularisation, for further growth and metastasis. Angiogenesis and remodeling are required for the development of the tumor microcirculation[7]. Neoangiogenesis results from the proliferation, sprouting, and migration of endothelial cells within normal tissues adjacent to the tumor. Studies have shown that varying types of vascularisation are evident in melanomas[8]. Angiogenesis is predominant in pigmented melanomas, neovascular channels arising from pre-existing stromal vessels at the invasive margins. In the aggressive amelanotic melanomas, embryonic vasculogenesis predominates[9].

Melanomas show a wide variation in pigmentation, some tumors showing heavy pigmentation, while some are

amelanotic and others show nodules varying from deeply pigmented to amelanotic. The present study evaluates whether this variation is due to a clonal difference or due to a reprogramming of the component tumor cells and the possible role of angiogenesis and tumor vascular interactions.

Results

Morphologic Patterns
General tumor

Pigmented areas show marked anisocytosis and anisonucleosis[Figure 1a]. Pleomorphism is prominent with cells varying in shape from spindloid to rhabdoid to tadpole shaped. Variable mixtures of both spindle and epithelial cells are seen. Cells with other morphology are observed comprising of round cells and balloon cells. Mononucleate and multinucleate giant cells with 10-12 nuclei are seen in some areas. Giant cells with peripherally placed multiple nuclei are also observed as are mononucleate giant cells with open chromatin.

The epithelioid cells are large cells with polygonal outlines, eosinophilic cytoplasm with round to oval vesicular nuclei arranged in a nested pattern. The fascicles and nests are separated by thin or dense connective tissue. The nuclear appearance too varies with some nuclei being dense and hyperchromatic with an indistinct nucleolus. Occasional tumors show areas with small round cells with scanty cytoplasm and dense nuclei are arranged in a rosettoid pattern mimicking primitive neuroectodermal tumors.

Amelanotic areas show a diffuse pattern of continuous sheets of fairly uniform cells [Figure 1b]. Balloon cells are identified by their abundant, clear cytoplasm, relatively little nuclear atypia and scanty pigment; and are seen with epithelial cells[10-13]. The nucleus is large and vesicular with chromatin scattered in irregular clumps. This type of nucleus is mostly associated with a large and prominent nucleolus.
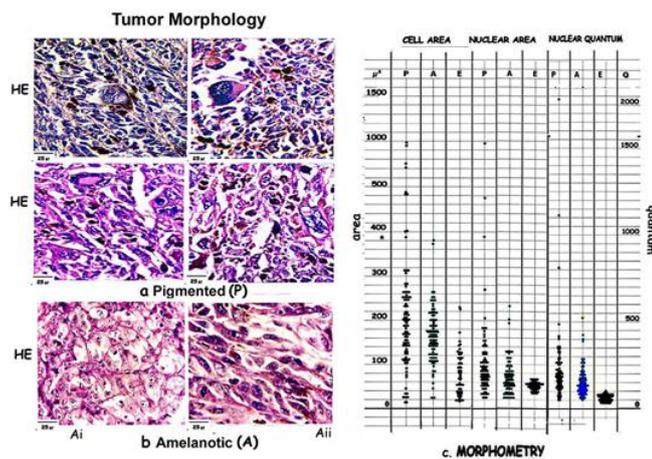

Figure 1: Composite figure showing morphological features of [a] Pigmented areas [P] with marked pleomorphism, [b] Amelanotic areas [Ai, Aii] with uniform cells. [c] Scatter diagram compares cell and nuclear areas and nuclear density in pigmented [P] amelanotic cells [A] and epidermal melanocytes [E].
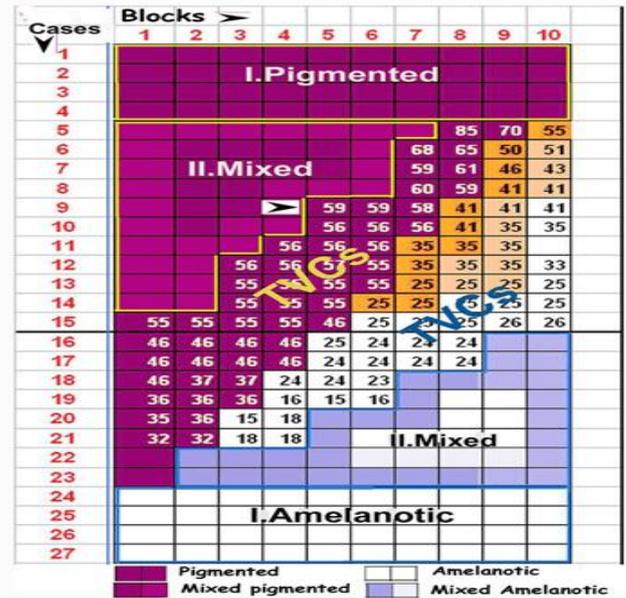

Figure 2: Grid showing blocks arranged in order of pigment levels in the cases studied. General pigmented areas are marked brown [▢[, 40 blocks in pigmented tumors and 44 in mixed tumors. Poorly pigmented amelanotic areas are white [▢▢], 40 blocks in amelanotic tumors and 43 in mixed tumors. 103 blocks from the tumor-stroma interphase, 51 from pigmented and 52 from poorly pigmented nodules have been marked with the number of TVCs in each.

Mixed tumors are formed of multiple variegated nodules some showing heavy pigmentation, others graded peripheral pigmentation and some amelanotic as arranged in the grid[Figure 2, 3].
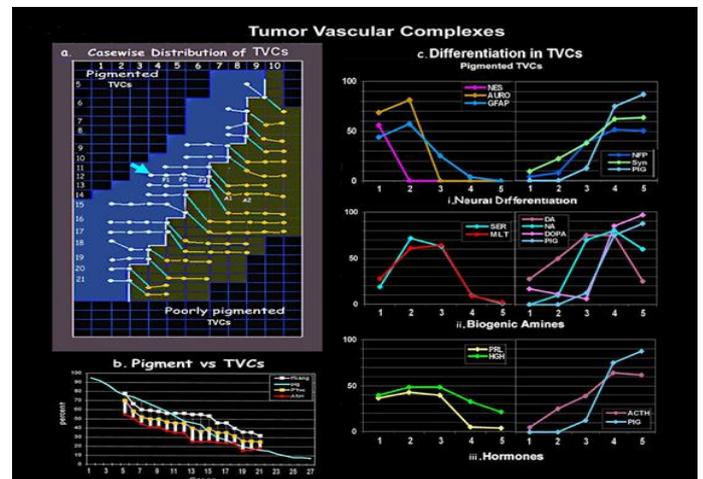
Figure 3: [a] Grid shows the case wise distribution of TVCs in pigmented and poorly pigmented nodules of mixed tumors. Arrow indicates the case where morphometric measurements and patterns of differentiation in 5 groups of TVCs, P1, P2, P3, from pigmented and A1 and A2 from amelanotic nodules, have been compared with pigmented, amelanotic, and epidermal parameters. [b] Graph depicting the association of pigment levels with total angiogenesis and TVC formation in melanotic and poorly pigmented nodules. [c] Comparative graphs show organized differentiation [i.neural, ii. biogenic amines and iii. hormone] in the mantle zone of pigmented TVCs.

Morphometry

Morphometry highlights the variations in pigmented and amelanotic tumors. The cell and nuclear areas, and the DNA quantum have been compared with epidermal melanocytes [Figure 1, Table 1]

Table 1: Cell and nuclear areas and the range in P and A are compared with normal epidermal melanocytic values. P shows marked pleomorphism of cells with a wide range of values being 1419.1μ², while A is uniform 354.8μ² and shows near epidermal values 207μ². Nuclei show a similar trend P showing the greatest range of 967.7μ², A 167.7μ² and E 40.3μ².

	cell area			nucleus		
	min	max	range	min	max	range
epidermal	18μ²	225μ²	207μ²	7.1μ²	47.4μ²	40.3 μ²
pigmented	12.9μ²	1431.9μ²	1419.1μ²	25.6μ²	993.3μ²	967.7μ²
amelanotic	25.8μ²	380.6μ²	354.8μ²	25.8μ²	193.5μ²	167.7μ²

General Tumor[Table.1]
Pigmented Areas

The pigmented areas show marked variation in cell and nuclear size, and nuclear content. Cell areas vary from a minimum of 12.9μ² to a maximum of 1431.9μ²: [range: 1419.1μ²]. Nuclear areas vary from 25.6 to 993.3μ² [range: 967.7μ²] and nuclear DNA from 0.0551 - 2.3046 [range 2.2495].

Amelanotic Areas

In contrast the values in the amelanotic tumors are closer to the normal epidermal values with near normal variation in cell and nuclear size and DNA content. Cells vary from a minimum of 25.8μ² to 380.6μ², a range of 354.8μ², Nuclear areas vary from 25.8μ² to 193.5μ², a range of 167.7μ² and nuclear DNA varies from 0.0504 - 0.5209: range 0.4705.

Epidermal Melanocytes

Cell areas vary from 18μ² - 225μ² with a range of 207μ², nuclear areas vary from 7.1μ² – 47.4μ² the range being 40.3μ² and nuclear DNA ranges from 0.0344-0.1026 [0.0682] in epidermal melanocytes.

Mitotic Activity [Figure 4]
All counts were done on serial PCNA and Ki67 stained sections.
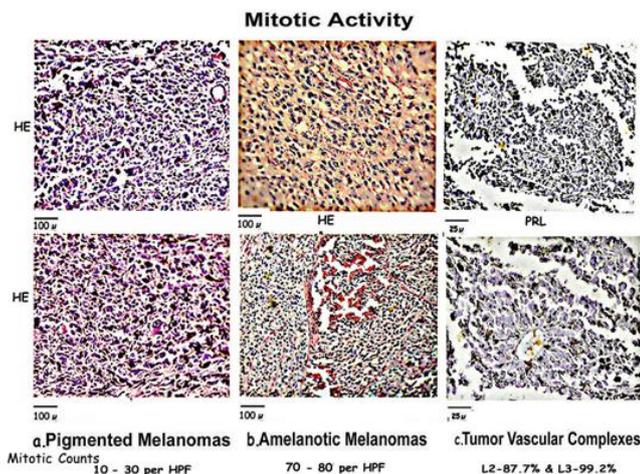

Figure 4: Composite figure compares mitosis in [a] Pigmented areas which show marked pleomorphism and abnormal mitosis; [b] Amelanotic areas having synchronized near normal mitosis with surrounding uniform cells; and [c] TVCs which show normal bipolar mitosis in the 2nd and 3rd layers of the mantle zone.

Pigmented Areas [Figure 4a]

Mitotic figures are prominent in most areas throughout the pigmented tumors more so nearer the margins varying from 10 to 30 per hpf or more. A prominent number of highly abnormal tripolar or multipolar and aneuploid nuclei, with very occasional bipolar mitotic figures can be seen.

Amelanotic Areas [Figure 4b]

Amelanotic tumors show a very large number of near normal mitotic figures 70 to 80 per hpf with intervening areas showing very few indicating waves of synchronization of mitosis with rapid proliferation. These melanomas, composed of uniform cells, show few abnormal mitotic figures.

Mitosis in TVCs [Figure 4c]

Mitosis is mainly concentrated in the layers L2 and L3 903 TVCs out of 1030 [87.7%] showed mitotic figures in L2. 1022 TVCs out of 1030 [99.2%] showed mitotic figures in L3 compared to 21% TVCs [216/1030] had very occasional mitosis L4, with 1383 out of 13824 cells [10%] in L4. L1 and L5 do not show significant numbers of mitotic figures. The mitotic figures in the TVCs are predominantly bipolar and normal in appearance.

Patterns of Differentiation [Figure 5, Table 2, 3]

The expression of neural markers, pituitary hormones; indoleamines; catecholamines and matrix proteins by melanocytes in association with pigmentation and morphological variation has been examined in this section.
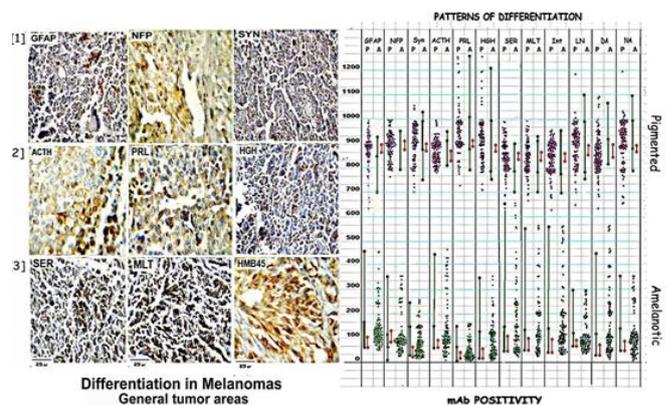
Figure 5: Shows differentiation in general tumor areas as seen by the positivity for GFAP, NFP, & Synaptophysin in[1]; ACTH, PRL & HGH in[2]; Serotonin, Melatonin & HMB45 in[3]. The attached scatter diagram shows high positivity of all markers in pigmented areas and very low positivity in amelanotic areas.

Table 2: shows the ranges of GFAP, NFP, & Synaptophysin; ACTH, PRL & HGH; Serotonin, Melatonin, DA, NA and the matrix proteins, LN5 & integrin positivity in pigmented and amelanotic areas in fully pigmented versus amelanotic tumors. The ratios show the high differentiation in the pigmented as compared to amelanotic areas which form polar groups.

I. Polar	Pigmented		Amelanotic			
mAb	min	max	min	max	mAb	ratio
GFAP	860	890	60	81	GFAP	12.4:1
NFP	870	910	58	78	NFP	13.5:1
Synp	870	890	31	61	Synp	19.2:1
ACTH	829	868	59	89	ACTH	11.8:1
PRL	891	909	10	29	PRL	44.8:1
HGH	869	888	19	56	HGH	22.7:1
SER	831	850	41	110	SER	9.6:1
MLT	829	849	40	99	MLT	10.8:1
LN5	860	880	59	79	LN5	13:01
inte	827	849	40	100	inte	10.8:1
DA	841	899	23	60	DA	19.8:1
NA	860	890	56	74	NA	14.5:1

mAb +ve cell counts

Positive Cell Counts [Figure 5, Table 2, 3]

All pigmented areas were positive for the neural markers, the three neurohormones, catecholamines, indoleamines as well as the matrix proteins. Positive cell counts showed a range of 698-1299 positive cells per block in 84 blocks from pigmented nodules as shown in the scatter diagram and values in [Table 3]. Positivity for all the markers is low or absent in amelanotic areas. Positive cells counted in 83 blocks from amelanotic nodules showed a range of 0-649 cells per block. Thus the total range of immune positivity is 70% to 100% in pigmented areas and 0% to 65% in amelanotic areas.

Differentiation in pigmented and amelanotic nodules were assessed and compared in purely pigmented and amelanotic tumors and mixed tumors.

In the Polar Group [Figure 5 Table 2 Polar] Pigmented nodules show a total range of 827-909/1000 positive cells [82.7%-90.9% positivity]. Integrin/SER show minimum: 836/838 cells/1000 while PRL shows a maximum positivity of 899.6 cells/1000, the overall positivity being 87%.

In comparison amelanotic nodules show a range of 10-110/1000 cells a positivity of 1% - 11%. Minimum positivity is seen with PRL: 201 positive cells/10hpf and maximum with SER: 872 positive cells/10hpf the reverse of pigmented nodules; the overall positivity is 605 /10hpf [61%]

In comparison in the Mixed Group [Figure 5 Table 3] Pigmented nodules show a total range of 698-1299/1000 or 69.8%-100% positivity. SER show minimum: 838 cells/10hpf while PRL shows a maximum positivity of 1018 cells/10hpf, the overall positivity being 904 cells/10hpf or 90% cells showing positivity in 10hpf. Amelanotic nodules show a total range of 0-649 positive cells in 10hpf) a percentage positivity of 0%-65%. The minimum positivity is seen with PRL: 77 positive cells/10hpf and maximum with SER: 323 positive cells/10hpf the reverse of P; the overall +ve: 237 positive cells/10 hpf [24%].

Table 3: shows the ranges of positive cell counts of neural markers; pituitary hormones; biogenic amines & matrix proteins in pigmented and amelanotic areas in mixed tumors. The ratios show the high differentiation in the pigmented versus amelanotic areas as seen in polar groups.

II. Mixed	Pigmented		Amelanotic			
mAb	min	max	min	max	mAb	ratio
GFAP	698	899	101	453	GFAP	3.4:1
NFP	790	950	90	354	NFP	3.1:1
Synp	900	1025	61	253	Synp	6.03:1
ACTH	851	938	140	443	ACTH	2.8:1
PRL	920	1299	0	151	PRL	13.2:1
HGH	886	1206	39	343	HGH	6.12:1
SER	783	894	91	649	SER	2.6:1
MLT	775	898	103	553	MLT	2.9:1
LN5	833	1100	101	298	LN5	4.7:1
inte	777	948	102	552	inte	2.7:1
DA	850	1066	111	443	DA	3.1:1
NA	840	1091	89	354	NA	2.9:1
mAb +ve cell counts						

Ratios [Figure 5 Table 3]

The overall P: A ratio in Group I is 14.3:1 [max: PRL: 44.8:1; min: SER: 9.6:1;] where as the ratio is 3.8:1 [max: PRL: 13.2:1; min: SER: 2.6:1;] in Group II. Thus in both groups pigment nodules show higher positivity, Group I showing a much larger difference.

Thus the pigmented and amelanotic areas form polar groups with extreme divergence in morphology, morphometric parameters and differentiation.

## Tumor Vasculature [Figure 6]
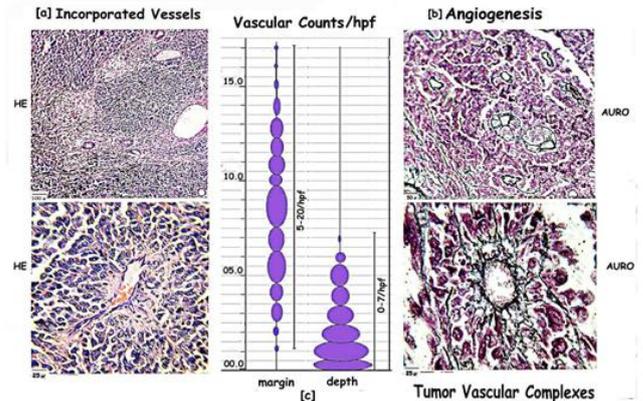
Figure 6: Composite picture of tumor vasculature within general areas and at invading margins, showing: [a] Incorporated vessels [INC] within fibrous stroma of the tumor show branching and sprouting. The surrounding tumor cells are pleomorphic, with prominent pigment and abnormal mitosis. There is no interaction as seen at the advancing edge of the tumor. [b] Angiogenic vessels elicited by the tumor interact with the tumor cells to form TVCs which show organized differentiation within the mantle zone. [c] Scatter diagram highlighting the high vascular counts in the marginal 2hpf as compared with areas in the depth the maximum being 20/hpf.

Incorporated Vessels [INC] [Figure 6a]

General pigmented areas show incorporated vessels. Blood vessels incorporated within the fibrous tissue of the tumor show sprouting and branching. Angiogenic vessels seen at the marginal interphase is not apparent. The surrounding tumor cells remain chaotic with no definite organization as seen with the marginal tumor vascular interaction.

Angiogenesis from normal stromal vessels at the advancing margin of tumor:

Vascular counts [Figure 6c]

The margins show a maximum of 20 bv/hpf and a minimum of 5 bv/HPF while areas of main tumor growth show a maximum of 6 bv/HPF and a minimum of 0 bv/HPF are observed. Thus angiogenesis is significantly higher at the margins as compared to that within the tumor [5hpf].

Tumor Vascular Interaction

The adjacent pre-existing blood vessels within the stroma extend endothelial tubes which cannelise and enter the tumor margins. The tumor cells interact with the angiogenic vessels to a depth of 2hpf to form a tumor-vascular-complex [TVC] with a perivascular mantle zone [PMZ] of 5 to 6 cell layers labeled L1-L5. [Figure 6b][6]

Distribution of TVCs [Figure 2, 3a]

The TVCs from both pigmented and amelanotic nodules are counted in 5 random hpf along the tumor margin in

contact with the surrounding stroma as given in the grid. Serial sections are treated as given in Methods.

Pigment vs Angiogenesis

Grid shows the number of TVCs in pigmented [P] vs amelanotic [A] nodules at the tumor/stroma interphase the [Figure 3a] showing the percentage in each case for comparison. Each hpf at the marginal zone has a potential for 20 TVCs, and 100 in 5hpf expressed as a percentage[14].

There are a total number of 4182 TVCs in the 103 blocks, 2646 [63.3%] in the pigmented and 1536 [36.7%] in amelanotic nodules. The 51 pigmented nodules show 85 to 32 TVCs while the 52 amelanotic contain 55 to 15 TVCs. On comparison pigmented nodules show higher number of TVCs in total, as well as within each tumor, there being a graded decrease in relation to the level of pigment in each nodule [Figure 3b].

Differentiation in TVCs [Figure 3c, Table 4]

Nes positivity is seen in cells abutting on the lumen till the formation of 1 to 2 layers [56.25%], thereafter to be replaced by Auro [L1: 68.75%; L2: 81.25%] and GFAP positivity [L1: 43.75%; L2: 57.25%]. Nes/Aurophilic, and GFAP positive processes extend outward from this layer, to form a supporting frame-work for the extending layers of tumor cells.

Table 4: Differentiation in TVCs: A comparative table showing percentage positivity of neural, biogenic amines, pigment and hormones in pigmented and poorly pigmented TVCs, P showing 5 times the overall percentage positivity seen in A. Peak positivity in each has been highlighted. GFAP, Nes & Auro are positive in L1/L2, Indoleamines, HGH & PRL in L2/L3 and catecholamines pigment and ACTH in the outer layers.

Differentiation in TVC

Table 4

	P	Pigmented					Poorly Pigmented				
		1	2	3	4	5	1	2	3	4	5
N	NES	56.25	0	0	0	0	9.5	0	0	0	0
	AURO	68.75	81.25	0	0	0	5.5	2.8	0	0	0
	GFAP	43.75	57.3	25.5	3.8	0	1.4	10.5	3	0	0
	NFP	3.8	7.9	38.9	51.7	50.6	1.7	8.1	18.5	6.8	3
	Synapt	9.7	21.9	38	62.3	63.5	2	5.6	11.6	17.8	20
H	PRL	36.3	42.5	39.8	5	3.8	3	5	1	0	0
	HGH	39.8	48.6	48.7	32.8	21.4	22.5	0	2.5	0	0
	ACTH	5	25	39.1	64.2	61.6	0	0	2.4	4	6
B	SER	19.1	71.8	62.8	9.4	0.9	4	10.7	0	0	0
	MLT	27.5	60.9	64.1	8.6	1.6	1.2	3.6	0	0	0
	DOPA	17	11.4	6	84.9	96.9	0	0	0	21.5	1.5
	DA	27.5	50	75	75	25	2.7	15	24.3	24	14
	NA	0	10	70	80	60	0	5.6	26	28	21
	PIG	0	0	12.5	75	87.5	0	0	0	0.4	0.9

N: Neural Differentiation ; H: Hormones ; B: Biogenic Amines
ANOVA: Pairwise comparisons in TVCs layers:
• Neuro: GFAP/Nes are significantly higher than NFP/Syn in L1&L2 and significantly lower in L4&5 (p<0.001).
• Biogenic Amines: Indoleamines (SER/MLT) are significantly higher than catecholamines (DA/NA) in L1&L2; (p<0.001), while being significantly lower than catecholamines, DO & pigment L3, L4&L5 (p<0.001). DO positivity is highest in L4 (p<0.001). Pigment positivity peaked in L5 (p<o0001).
• Hormones: PRLJHGH are significantly higher than ACTH in L2&L3 (p<0.001) while significantly lower than ACTH in L4&L5.

Indoleamines are positive in L2/L3 associated with mitosis. Both serotonin [L2:71.8%; L3:62.8%] and melatonin [L2:60.9%; L3:64.1%] are positive in these layers. All three pituitary hormones are expressed by the proliferating melanoma cells. HGH [L2:48.6%; L3:48.7%] and PRL [L2:42.5%; L3:39.8%] are expressed in the inner three layers.

Catecholamines DA [L3:75%; L4:75%]/NA [L3:70%; L4: 81.25%] and the related enzyme DO are positive in the layers L3/L4 & L5. Pigment [L4:75%; L5: 80%] and ACTH [L4: 64.2%; L5: 61.6%] are expressed in the 4th and 5th layers, where mitotic figures are scant, associated with NFP [L4: 51.7%; L5: 50.6%] and Syn [L4: 62.3%; L5: 63.5%] positivity.

Thus there is a regimented neurogenesis in the TVCs, initiated by endothelial tubes interacting with tumor cells beginning with glial differentiation followed by indoleamines and HGH/PRL in the middle layers and further by catecholamines and ACTH in the outer layers. Differentiation is proportionate to the level of pigmentation.

All markers are higher in pigmented TVCs as compared to those from poorly pigmented areas as illustrated in [Table 4], pigment positivity being 60 times higher MLT/HGH positivity, 20 times; ACTH positivity 11 times; PRL positivity is 8 times; NFP/SER positivity is 7 times; DO positivity is 6.5 times; GFAP positive being 6 times; Syn positivity is 4 times greater.

On Anova Analysis GFAP is significantly higher than NFP/Syn in L1&2 [(P = 0.030). F: 13.885] and significantly lower in L4&5 [(P = 0.004). F: 59.878 in L4&5]. Tukey test: All Pairwise Multiple Comparison Procedures: Comparison: P P<0.050: GF vs. NFP:0.031 Yes; Syn vs. GF:0.004 Yes

Morphometry [Figure 7 Table 5]

Since mitosis appears near normal in poorly pigmented areas and in TVCs, morphometry was done to compare the morphometric parameters of pigmented, poorly pigmented from general areas and the mantle zone of TVCs with normal epidermal melanocytes. 5 random TVCs were taken from three pigmented [P1, P2 & P3] and 2 poorly pigmented areas [A1 & A2] from the same case for comparison [Table 5].
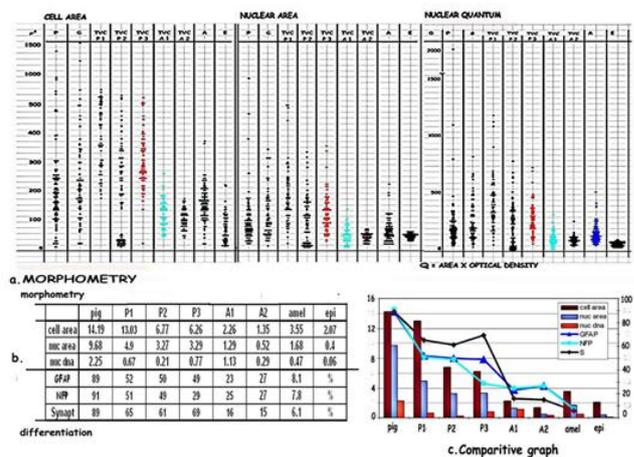

Figure 7: [a] Scatter diagram comparing morphometric parameters in P, A and TVCs from pigment and poorly pigmented nodules. There is a graded reduction in cell, nuclear size and DNA from the pigmented nodules, to pigmented TVCs, P1, P2, P3, amelanotic TVCs, A1, A2 and amelanotic nodules. [b] Table comparing morphometric parameters and differentiation from pigmented to amelanotic areas. [c] Comparative graph highlights the gradual loss of morphometric parameters and stepwise differentiation from melanotic to amelanotic areas indicating reprogramming of component cells. Poorly pigmented TVCs and amelanotic areas show near normal values which match those of epidermal melanocytes

Table 5: shows a gradation in morphometric values in TVCs, cell areas ranging from 1302.9μ² in P1, to 135.4μ² in A2, nuclear areas from 490.2μ² in P1 to 51.6μ² in A2, pigmented TVCs having parameters closer to pigmented areas while amelanotic TVCs are closer to amelanotic: cell areas and Epidermal values (40.3μ²).

	cell area			nucleus		
TVC	min	max	range	min	max	range
P1	180.6μ²	1483.5μ²	1302.9μ²	25.8μ²	516μ²	490.2μ²
P2	12.9μ²	690.2μ²	677.3μ²	12.9μ²	341.8μ²	326.9μ²
P3	25.8μ²	651.5μ²	625.7μ²	32.3μ²	361.2μ²	328.9μ²
A1	51.6μ²	277.4μ²	225.8μ²	12.9μ²	141.9μ²	129μ²
A2	45.2μ²	180.6μ²	135.4μ²	25.8μ²	77.4μ²	51.6μ²
Epidermal	18μ²	225μ²	207μ²	7.1μ²	47.4μ²	40.3μ²
Tumor Vascular Complex						

Cell areas of TVCs show a range of 1302.9μ² in P1, 677.3μ² in P2, 625.7μ² in P3. In comparison, cell areas range from 225.8μ² in A1 to 135.4μ² in A2. Nuclear areas vary from 490.2μ² in P1, 326.9μ² in P2; and 328.9μ² in P3. The amelanotic TVCs A1 and A2 show a range of 129μ² and 51.6μ². DNA content [Q] varies from 0.6686 in P1; 0.2134 in P2 while 0.7706 in P3. Q ranges from 1.1307 in A1 and 0.2944 in A2. The greatest variation in cell size, nuclear size and content is in P1 and the pigmented TVCs with a gradual reduction to the lowest in the amelanotic A2.

Epidermal melanocytes: cell areas range: 207μ²; Nuclear areas range: 40.3μ²; Nuclear DNA range: 0.0682.

The cell and nuclear sizes and range show a gradual reduction from pigmented to amelanotic TVCs as can be seen in [Figure 7a] in the scatter diagram and [Table 5], the parameters being near normal in those from poorly pigmented areas. The component cells of the mantle zone of TVCs are more uniform matching normal epidermal melanocytes, those from pigmented nodules showing a greater scatter due the presence of glial cells. This is associated with a similar reduction in differentiation as depicted in the comparative graph 7c.

Progression and Fate of TVCs [Figure 8]
The progression and fate of the TVCs was studied in depth in view of the gradation seen in the differentiation and morphometric parameters from pigmented to amelanotic nodules. Serial sections are used to follow the progression and growth of TVCs beyond 2 hpf from the stromal margins. Stacks of serial sections are used for 3D constructs and are drawn out as a collage [Figure 8] to follow the growth and fate of the TVCs and to study vascular interactions within and around the growing tumor.
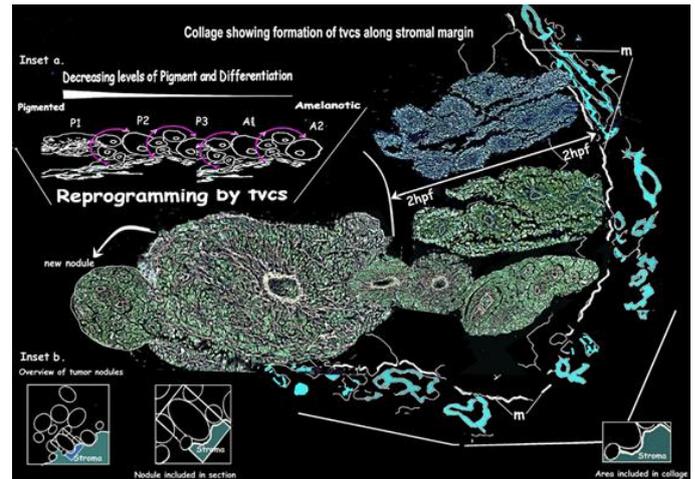

Figure 8: 3D rendering of a collage tracing extension of angiogenic vessels and the progression of TVCs beyond the marginal 2hpf: [m] shows the marginal zone between the advancing tumor and the pre-existing stroma. The upper part shows several vessels with growing TVCs from a section stained with mAb PRL. The lower part is from gold impregnated serial sections tracing the vessel and TVC beyond 2hpf. As it enlarges a second wave of angiogenesis with TVC formation occurs as the margin is contacted once again.
Insets: [a] Summary diagram of cyclical angiogenesis and TVC formation, depicting the process of reprogramming of highly pigmented cell groups to uniform near normal amelanotic cells.
[b] Diagramatic overviews of the tumor area sampled.

Reprogramming and Remodeling [Figure 8 Table 5]
Angiogenesis and TVCs are directly proportionate to the level of pigmentation [Figure 6b]. Contact of pigmented tumor margins with normal stroma elicits angiogenesis from the adjoining pre-existing normal stromal vessels. As the angiogenic vessel grows beyond 2 hpf the mantle layers continue to increase to form enlarging nodules with pigmented peripheral layers, the overall pigment being less than the general tumor. When these contact the stromal margin angiogenesis and TVC formation is elicited in proportion to the pigment level. There is a reduction in pigment at each cycle. This cycle repeats itself until differentiated pigmented cells are depleted. With the absence of angiogenesis in the poorly pigmented TVCs the organized growth of the layers is lost and sheets of characteristic amelanotic cells are formed.

Discussion

The above study highlights the role of angiogenesis in remodeling and reprogramming in melanomas. Nodules of varying sizes and pigmentation are seen side by side in mixed tumors. The general melanotic and amelanotic areas are in sharp contrast forming polar groups [Figure 1, 5]. The pigmented areas show prominent pleomorphism, marked variation in cellular and nuclear size, high levels of chaotic differentiation, and prominent abnormal mitosis. In contrast, amelanotic areas show uniformity in cell morphology, cell and nuclear size tend to be near normal epidermal parameters, differentiation being low with near normal synchronized mitosis [Figure 4].

The remodeling of preexisting vessels surrounding the growing tumor active sprouting and branching of these vessels helps meet the metabolic demands of tumor cells[15]. Angiogen-

esis begins by focal reduction of vascular intercellular interactions in preexisting ones and increased interactions between vascular cells and the extracellular matrix [ECM]. The tumor cells at the advancing edge produce LN5 and integrin $[\alpha_5\beta_1]$ both of which are involved in the dissolution of the local ECM to allow the cells to move forth further[9]. Continuous stimulation of vessel outgrowth expands the vascular compartment of the growing tumor.

Melanomas show incorporated vessels[INC], vasculogenic mimicry[VM], and angiogenesis[9]. Angiogenesis is seen at the tumor-normal stroma interphase and is proportionate to the pigment levels, very low angiogenesis being elicited in amelanotic areas. Tumor induced angiogenic tubes enter the margins, interact with the tumor cells, and form 3D tumor-vascular-complexes[TVCs] consisting of a central vessel and a perivascular mantle of cells[PMZ]. The component cells are more uniform, with normal mitotic figures and regulated organized, neural differentiation.

The melanoma cells express GFAP[16] and nestin positivity[17,18] as well as aurophilia assessed by the modified gold impregnation technique[9] which identifies characteristics of radial glia, on interaction with the endothelial tubes[9,14].These cells proliferate and differentiate into cells positive for neuronal markers and thus function as multipotent astrocytic stem cells[MASC] simulating neurospheres in cultures[19-26]. The presence of radial glial MASC during embryogenesis has been described in several studies[16-26].

There is a reciprocal paracrine interaction between astrocytes, endothelial cells and ependymal cells. Astrocytes and neurons release vascular endothelial growth factor [VEGF165] to elicit a burst of mitotic angiogenesis. The activated microvascular cells produce brain-derived neurotrophic factor BDNF[27,28]. Neuronal progenitor and mitotic endothelial cells are spatially associated in foci of concurrent angiogenesis and neurogenesis[29].

The steps of progression, from radial glial to neuronal cells, in the peri-mantle zone [PMZ] is similar to the differentiation in invitro neurospheres and early neuro-embryogenesis. The newly-generated neurons from astrocyte-like stem cells, can assume or revert to an astrocytic phenotype[20,23]. Neurons transit through an "asteron" (neuron/astrocyte hybrid) to shift into cells with astrocyte characteristics in differentiating primary floating neurospheres. These asterons coexpress a variety of neuron and astrocyte proteins and genes.

Earlier studies have identified the presence of biogenic amines in melanocytes[2-4]. Synaptophysin labels small synaptic like microvesicles (SLMV), which are positive for biogenic amines. SLMVs are present in neuroendocrine cells such as the pituitary and adrenal medulla. During embryogenesis, the serotoninergic and dopaminergic neurones arise from common progenitors stem cells with enzymes cat-1 & cat- 4 and bas-1[30-31]. As development progresses, the serotoninergic cells remain at the brain stem and the post-mitotic dopaminergic cells proceed to the midbrain SNC. This feature is replicated in the TVC, with indoleamines positivity in middle layers and catecholamines in the outer layers. All three pituitary hormones are expressed by the proliferating melanoma cells. HGH and PRL are expressed in the middle layers associated with mitosis, while ACTH is positive in the outer layers[32].

Mitosis is mainly concentrated in the middle layers of the TVCs. Outer layers do not show significant numbers of mitotic figures. The mitotic figures in the TVCs are predominantly bipolar and normal in appearance as compared to the abnormal mitotic figures seen in the surrounding tumor. Polarity and asymmetric mitosis are evidenced by the generation of indoleaminergic and catecholaminergic cells in different layers of the TVCs in response to angiogenesis.

Cell diversity is generated by essential cell polarity required for the proper function of most differentiated cell types. Apical/basal polarity in mitotic neuroblasts, results from asymmetrical division to generate an apical neuroblast and a smaller basal ganglion mother cell (GMC). The GMC undergoes one subsequent cell division to generate neurons or glia[33, 34].

TVC counts are proportionate to pigment levels in association with level of angiogenesis, the pigmented areas showing higher counts as compared to poorly pigmented areas. TVCs taken from a single tumor from pigmented to amelanotic nodules shows a gradation of neurogenesis, the pigmented showing prominent differentiation, with the poorly pigmented showing very low neurogenesis [Figure 3b].

The cell and nuclear size show a gradual reduction from pigmented to amelanotic TVCs, parameters being near normal in those from poorly pigmented areas. The component cells of the mantle zone of TVCs are more uniform matching normal epidermal melanocytes, those from pigmented nodules showing a greater scatter due the presence of glial cells [Figure 7 Table 5]. These findings suggest that TVC formation and angiogenesis are linked with melanotic to amelanotic transition. Formation and progression of TVCs has been studied to assess this possibility [Figure 8].

The formation and fate of TVCs is elucidated by 3D constructs [Figure 8] by tracing individual vessels beyond marginal 2 hpf through serial and contiguous sections. The outer layers of the enlarging TVCs continue to have pigment at the margins but less within the core around the vessel. Nodules of different sizes are formed with varying levels of pigment. When these come into contact with the stroma a further wave of angiogenesis occurs, elicited by the peripheral pigmented cells this time forming TVCs within the margins of the TVC generated nodules.

This cyclical process continues with differentiation and pigment diminishing with every cycle. This is well illustrated by the comparative differentiation within TVCs in pigmented and poorly pigmented zones within the same tumors. At this stage the cells continue to proliferate and enlarge into amelanotic nodules and further into sheets of amelanotic cells replacing the pigmented areas. This brings out interesting features of TVC progression leading to a reprogramming and remodeling of the tumor, which is gradually replaced by amelanotic cells.

In comparison, in cell cultures, differentiated somatic cells can be reprogrammed to a pluripotent state by overexpression of four transcription factors Oct4, Sox2, Klf4, and c-Myc [OSKM] and Nanog[35-41].The reprogramming process[36,42, 43] generates iPSCs that resemble embryonic stem cells [ESCs].

Vasculogenesis, occurs with the formation of blood islands in the extra embryonic yolk sac during embryogenesis[7]. An inner layer of primitive hematopoietic cells and a peripheral population of angioblasts differentiate into endothelial cells. A similar process occurs in the amelanotic melanoma giving rise to hemopoeitic cells that normally derive from germ layers other

than the neuroectoderm and neuralcrest[44-46].

Embryonic microenvironments influence development of neuronal stem cells[47]. Similarly multipotent tumor cells, fate and plasticity of adult cell are influenced by the microenvironment[48]. Multiple cell types which originate from the highly invasive neural crest cell population of the vertebrate embryo can be reprogrammed by simulating a natural environment in 3D organ culture[47-51].

The present observations indicate that an embryonic microenvironment is created in the mantle zone of TVC around the angiogenic vessel, arising from pre-existing normal stromal vessels, to induce and recapitulate early embryonal neurogenesis of indoleaminergic and catecholaminergic cells. The angiogenic vessel confers a polarity to the interacting tumor cells resulting in a stepwise manner replacing the highly pleomorphic pigmented melanotic tumor cells by uniform, amelanotic tumor cells which behave like embryonal stem cells as is evidenced by the development of vasculogenic spaces[9].

Clinical and Therapeutic Significance

The present study outlines the role of angiogenesis in remodeling/reprogramming in melanomas. Anti-angiogenesis therapy has been used successfully in the treatment of a significant number of melanomas. It has been demonstrated by Griffioen and colleagues[52-56], that harmful endothelial cell anergy can be counteracted by inhibitors of angiogenesis. In the early phases of tumor growth angiogenic TVC result in the replacement of pigmented nodules by amelanotic nodules as described above. This can be inhibited by anti-angiogenesis therapy. The present study highlights the importance of anti-angiogenesis therapy before extensive amelanotic change occurs, capable of vasculogenesis resulting in resistance to anti-angiogenesis therapy. In view of the varying types of vascularisation seen in melanomas, the therapeutic strategies have also to target the self propagating vascular networks within the tumor, not involving the angiogenic pathways.

Material and Methods

Nodular melanomas in the vertical growth phase [VGP] were received from the Cancer Surgery Unit of Safdarjung Hospital, New Delhi, fixed in cold [4°C] 10% formol glutaraldehyde. The formaldehyde-glutardehyde cold fixation retains the morphology, gives crisp staining and efficient immunohistochemical staining both in frozen as well as paraffin sections. The same blocks can be subjected to electron microscopy as well. 10 nodules were sampled from each of 27 tumors, to make a total of 270 blocks, in the ratio of pigmented to poorly pigmented areas in each tumor. As the specimens were received and sampled the blocks were arranged in a grid, according to the pigment level which varied between 7% - 95% [Figure 2]. 20 to 40, 5µm thick serial frozen and paraffin sections of each block were maintained under refrigeration at 4°C for the following:

Histochemistry: HE, PAS, combined reticulin+gold impregnation for aurophilia[10]. Gold chloride sublimate specifically and exclusively stains astrocytes [confirmed by GFAP and nestin positivity] which stain intensely black. Reticulin is seen as a network of fine fibrils and the vascular basement membrane;

Enzyme histochemistry: dopa oxidase, tyrosinase and monoamino oxidase methods;

Immunohistochemistry: using the Avidin/ Biotin system[11-13].

The amelanotic melanocyte has been identified by the specific melanocyte markers HMB-45 and S-100 protein. The expression of neural markers, nestin [Nes], glial fibrillary acidic protein [GFAP], neural fibrillary protein [NFP] and synaptophysin [Syn]; pituitary hormones, adrenocorticotropic hormone [ACTH], prolactin [PRL], human growth hormone [HGH]; indoleamines [serotonin, melatonin]; catecholamines [DA, NA, dopa and pigment] and matrix proteins [LN5, integrin] were examined. As negative control all slides included a serial section stained with no mAb. The same mAb were used simultaneously against known positive sections from human skin as positive controls.

[**Immuno Chemicals:** GFAP: BioGenex Lab: Polyclonal; NFP: BioGenex Labs: Monoclonal; Synaptophysin: BioGenex Labs; Monoclonal; Serotonin: BioGenex Labs: Monoclonal; Melatonin: BioGenex Labs: Monoclonal; Adrenocorticotropic Hormone [ACTH]: Dako Pat kits: Polyclonal; Prolactin [PRL]: Dako Pat kits: Polyclonal; Human Growth Hormone [HGH]: Dako Pat kits: Polyclonal; LN5 [Laminin 5]: Kappa Zymed: Monoclonal; Integrin $_5$ $_1$: Dako Pat kits: Monoclonal].

Morphology and Morphometry

Morphology and morphometry were assessed on HE sections. Morphometric analysis of cell and nuclear size and nuclear density was done using a Semi-automated Zeiss Morphomat, Scion Image of NIH and a Reichert Cyto spectrophotometer to compare the size and the nuclear parameters of tumor cells with normal epidermal melanocytes. The nuclear content was assessed as follows: Area of nucleus x optical density x 5 (tissue thickness) = DNA [Q]

Electron microscopy: routine and after en bloc stain for dopa.
The above methods were applied to:

a. General tumor areas and

b. Tumor Vascular Complexes [TVCs].

a. General Tumour Areas [Figure 2]

167 blocks, 84 pigmented and 83 poorly pigmented and amelanotic nodules have been included.

In Group I, 4 cases are pigmented and 4 amelanotic to include 40 pigmented and 40 amelanotic nodules/ blocks.

In Group II 19 cases are mixed showing both pigmented and amelanotic general nodules composed of 87 blocks, 44 melanotic and 43 amelanotic.

All counts were double blind observations made by two unrelated observers and the author. Counts and measurements were repeated three times at 6 monthly intervals to remove any bias.

Quantitation by Morphometric Analysis

Morphometric measurements of cell size and the nuclear parameters were done in 200 cells on random pigmented and amelanotic nodules in each tumor. Measurements are represented as scatter diagrams for comparison. 100 melanocytes from overlying normal epidermis serve as control [Figure 1, Table1]. Morphometric counts were done blinded to the category of the tissue block (pigmented or amelanotic or mixed). Mitotic Activity and morphology was assessed in pigmented amelanotic areas and TVCs [Figure 4]. Mitotic counts were done and compared in these areas on sections stained with PCNA and Ki67 both specific for mitotic cells.

Immunohistochemistry [Figure 5]

Positive cell counts, of each marker were entered into the grid. Positive cells per 1000 cells were counted in random 10 HPF per block for each marker in serial sections. The positive counts are presented as scatter diagrams, comparing pigmented and amelanotic areas in: Group I. [Table 2] Pigmented vs Amelanotic tumors; 4 pigmented and 4 amelanotic tumors including 80 blocks [40P/40A]; and 19 mixed tumors which include 87 blocks [44P/43A] [Group II] [Table 3]. Expression of various markers in these two groups has been compared.

Tumor Vasculature

Incorporated Vessels [INC] are seen in 84 general pigmented nodules away from the tumor stroma interphase. [Figure 6].

Angiogenesis from Normal Stromal Vessels at the Advancing Margin of Tumor

103 blocks from mixed tumors, 51 blocks from pigmented and 52 from poorly pigmented nodules [Figure 2] at the interphase between the tumor and surrounding preexisting stroma, have been included for the study. A large number of angiogenic vessels are seen within 2hpf of the tumor margin with a maximum of 20 vessels per HPF associated with TVCs. [Figure 6]. Vascular channels are counted at the tumor margins in each of the 103 blocks to a depth of two high power fields [HPF] and at a depth of 5 to 6 HPF within the tumor in 10 HPF [1030 HPF marginal and 1030 HPF within tumor]. Vessel counts were done on sections stained with nestin, PAS and reticulin stain.

Tumor-Vascular-Complexes [TVCs]

Endothelial tubes from normal stromal vessels interact with tumor cells to form tumor-vascular-complexes [TVCs]. The TVCs from both pigmented and amelanotic nodules are counted in 5 random HPF in each block along the tumor margin at the tumor-stromal interphase [out of a possible maximum of 100 vessels]. A total of 1030 TVCs formed around vessels in cross section were included in the study [Figure 3].

Immunohistochemistry [Figure 3c]

Neural marker positivity has been examined in the layers of the perimantle zone [PMZ] of tumor-vascular complexes [TVC] formed during angiogenesis and compared in pigmented and amelanotic nodules as well as in the TVCs [Table.4]. Positivity recorded and compared are from 5 random TVCs each, from 3 pigmented [P1, P2, P3] and 2 amelanotic [A1, A2] nodules in the same tumor [Figure 3a]

Morphometry [Figure 7]

The measurements are taken from each layer in 5 random TVCs in pigmented and amelanotic nodules in all tumors. Measurements recorded and compared here are from 5 random TVCs each, from 3 pigmented [P1, P2, P3] and 2 amelanotic [A1, A2] nodules in the same tumor marked with arrow in [Figure 6a, Figure 7, Table 5].

Progression and Fate of TVCs [Figure 8]

Stacks of serial and contiguous HE, mAb, reticulin stained and gold impregnation sections, are used to make 3D reconstructs of angiogenic vessels arising from pre-existing normal stromal vascular channels showing interaction with the advancing tumor. These channels are traced beyond the marginal

2hpf to follow the growth of the TVCs and to study vascular interactions within and around the growing tumor. Presence of pigment, a positive DOPA reaction, and HMB-45 positivity are criteria for diagnosis. In the absence of pigment a positive dopa reaction, HMB45 positivity and the presence of premelanosomes on electron microscopy [EM] is diagnostic of amelanotic melanomas. These criteria form the basis of diagnosing each tumor included in this study.

References

1. Kalcheim, C., Le Douarin, N.M. The Neural Crest. Cambridge University Press1999.

2. Iyengar, B., Misra, R. S. The reaction of dendritic melanocytes in vitiligo to the substrates of tyrosine metabolism. (1987) Acta Anat 129(3): 203-205.

3. Iyengar, B. Indoleamines and the UV-light sensitive photoperiodic responses of the melanocyte network: A biological calendar? (1994) Experientia 50(8): 733-736.

4. Iyengar, B. The UV-responsive melanocyte system: a peripheral network for photoperiodic time measurements. a function of indoleamine expression. (1998) Acta Anat 163(4): 173-178.

5. Rifkind, R. A., Richon, V. M., Marks, P. A. Induced differentiation, the cell cycle, and the treatment of cancer. (1996) Pharmacol Ther 69(2): 97-102.

6. Iyengar, B., Singh, A.V. Patterns of neural differentiation in Melanomas. (2010) J Biomed Sci 17: 87.

7. Risau, W. Mechanism of angiogenesis. (1997) Nature 386(6626): 671-674.

8. Zhang, S., Zhang, D., Sun, B. Vasculogenic mimicry: current status and future prospects. (2007) Cancer Lett 254(2): 157-164.

9. Iyengar, B., Singh, A. V. Embryonic Vasculogenesis in Nodular Melanomas and Tumour Differentiation. (2011) Pathol Oncol Res 17(3): 569-577.

10. Iyengar, B. Multipotent Astrocytic Stem Cells Identified During Angiogenesis in Melanoma. (2011) WebmedCentral 2(12).

11. Mikel UV: Advanced Laboratory Methods in Histology and Pathology. (1994) American Registry of Pathology, Armed Forces Institute of Pathology, Washington DC.

12. Pearse AGE: Histochemistry theoretical and applied. Vol II: Analytical Technology. (1985) Churchill Livingstone, London. 611-674.

13. Prophet, E. D., Mills, B., Arrington, J. B., et al. Laboratory Methods in Histotechnology. (1994) American Registry of Pathology.

14. Iyengar, B. Biogenic Amines and Tumor-Vascular interaction in melanomas. (2011) J Solid Tumors 1(2): 44-55.

15. Papetti, M., Herman, I. M. Mechanisms of normal and tumor-derived angiogenesis. (2002) Am J Physiol Cell Physiol 282(5): C947-C970.

16. Raju, T., Bignami, A., Dahl, D. In vivo and in vitro differentiation of neurons and astrocytes in the rat embryo. Immunofluorescence study with neurofilament and glial filament antisera. (1981) Dev Biol 85(2): 344-357.

17. Messam, C. A., Hou, J. Major, E. O. Coexpression of nestin in neural and glial cells in the developing human CNS defined by a human-specific anti-nestin antibody. (2000) Exp Neurol 161(2): 585-596.

18. Wiese, C., Rolletschek, A., Kania, G., et al. Nestin expression-a property of multi-lineage progenitor cells? (2004) Cell Mol Life Sci 61 (19-20): 2510-22.

19. Alvarez-Buylla, A., Garcia-Verdugo, J. M., Tramont, A. D. A unified hypothesis on the lineage of neural stem cells. (2001) Nat Rev Neurosci 2(4): 287-293.

20. Doetsch, F. The glial identity of neural stem cells. (2003) Nat Neurosci 6(11): 1127-1134.

21. Garcia, A. D., Doan, N. B., Imura, T. GFAP-expressing progenitors are the principal source of constitutive neurogenesis in adult mouse forebrain. (2004) Nat Neurosc 7(11): 1233-1241.

22. Goldman, S. Glia as neural progenitor cells. (2003) Trend Neurosci 26(11): 590-596.

23. Laywell, E. D., Kearns, S. M., Zheng, T., et al. Neuron-to-astrocyte transition: phenotypic fluidity and the formation of hybrid asterons in differentiating neurospheres. (2005) J Comp Neurol 493(3): 321-333.

24. Noctor, S. C., Flint, A. C., Weissman, T. A., et al. Dividing precursor cells of the embryonic cortical ventricular zone have morphological and molecular characteristics of radial glia. (2002) J Neurosci 22(8): 3161-3173.

25. Yelamanchili, S. V., Reisinger, C., Becher, A., et al. The C-terminal transmembrane region of synaptobrevin binds synaptophysin from adult synaptic vesicles. (2005) Eur J Cell Biol 84(4):467-75.

26. Zecevic, N. Specific characteristics of radial glia in the human fetal telencephalon. (2004) Glia 48(1): 27-35.

27. Goldfinger, L. E., Hopkinson, S. B., deHart, G. W., et al. The alpha3 laminin subunit, alpha6beta4 and alpha3beta1 integrin coordinately regulate wound healing in cultured epithelial cells and in the skin. (1999) J Cell Sci 112(Pt 16): 2615-2629.

28. Trikha, M., Timar, J., Zacharek, A., et al. Role for beta3 integrins in human melanoma growth and survival. (2002) Int J Cancer 101(2): 156-67.

29. Koistinen, P., Ahonen. M., Kähäri, V. M., et al. alphaV integrin promotes in vitro and in vivo survival of cells in metastatic melanoma. (2004) Int J Cancer 112(1): 61-70.

30. Hobert, O. How to make dopamine neurons: In: ebrief: Neural Stem Cells: The New York Academy of Sciences 2008; PMid:18629870 PM-Cid:2570047.

31. Wallen, A., Perlman, T. Transcriptional Control of Dopamine Neuron Development. (2003) Ann N Y Acad Sci 991: 48-60.

32. Iyengar, B. Hormone Expression in Melanomas Related to Tumor Angiogenesis. (2012) Journal of Solid Tumors 2(6): 36-45.

33. Doe, C. Q. Molecular markers for identified neuroblasts and ganglion mother cells in the Drosophila central nervous system. (1992) Development 116(4): 855-863.

34. Zhong, W. Diversifying neural cells through order of birth and asymmetry of division. (2003) Neuron 37(1): 11-14.

35. Hanna, J., Saha, K., Pando, B., et al. Direct cell reprogramming is a stochastic process amenable to acceleration. (2009) Nature 462(7273): 595-601.

36. Maherali, N., Ahfeldt, T., Rigamonti, A., et al. A high-efficiency system for the generation and study of human induced pluripotent stem cells. (2008) Cell Stem Cell 3(3): 340-345.

37. Niwa, H., Miyazaki, J., Smith, A. G. Quantitative expression of Oct-3/4 defines differentiation, dedifferentiation or self-renewal of ES cells. (2000) Nat Genet 24(4): 372-376.

38. Avilion, A. A., Nicolis, S. K., Pevny, L. H., et al. Multipotent cell lineages in early mouse development depend on SOX2 function. (2003) Genes Dev 17(1): 126-140.

39. Park, I. H., Lerou, P. H., Zhao, R., et al. Generation of human-induced pluripotent stem cells. (2008) Nat Protoc 3(7): 1180-1186.

40. Takahashi, K., Yamanaka, S. Induction of pluripotent stem cells from mouse embryonic and adult fibroblast cultures by defined factors. (2006) Cell 126(4): 663-676.

41. Mitsui, K., Tokuzawa, Y., Itoh, H., et al. The homeoprotein Nanog is required for maintenance of pluripotency in mouse epiblast and ES cells. (2003) Cell 113(5): 631-642.

42. Koche, R. P., Smith, Z. D., Adli, M., et al. Reprogramming factor expression initiates widespread targeted chromatin remodeling. (2011) Cell Stem Cell 8(1): 96-105.

43. Papp, B., Plath, K. Reprogramming to pluripotency: stepwise resetting of the epigenetic landscape. (2011) Cell Res 21(3): 486-501.

44. Bjornson, C. R., Rietze, R. L., Reynolds, B. A. Turning brain into blood: a hematopoietic fate adopted by adult neural stem cells in vivo. (1999) Science 283 (5401): 534-537.

45. Louissaint, A. Jr., Rao, S., Leventhal, C., et al. Coordinated interaction of neurogenesis and angiogenesis in the adult songbird brain. (2002) Neuron 34(6): 945-960.

46. Shima, D. T., Mailhos C. Vascular development biology: getting nervous. (2000) Curr Opin Genet Dev 10(5): 536-542.

47. Kulesa, J. C., Teddy, J. M., Postovit, L. M., et al. Reprogramming multipotent tumor cells with the embryonic neural crest microenvironment. (2008) Dev Dyn 237: 2657-2666.

48. Hendrix, M. J., Seftor, E. A., Seftor, R. E., et al. Reprogramming metastatic tumour cells with embryonic microenvironments. (2007) Nat Rev Cancer 4: 246-255.

49. Le Douarin, N. M., Dupin, E. Multipotentiality of the neural crest. (2003) Curr Opin Genet Dev 13(5): 529-536.

50. Postovit, L. M., Seftor, E. A., Seftor, R. E. B., et al. Influence of the microenvironment on melanoma cell-fate determination and phenotype. (2006) Cancer Res 66(16): 7833-7836.

51. Topczewska, J. M., Postovit, L. M., Margaryan, N. V., et al. Embryonic and tumorigenic pathways converge via Nodal signaling: role in melanoma aggressiveness. (2006) Nat Med 12(8): 925-932.

52. Dirkx, A. E. M., Egbrink, M. G. A., Castermans, K., et al. Anti-angiogenesis therapy can overcome endothelial cell anergy and promote leukocyte-endothelium interactions and infiltration in tumors. (2006) FASEB J 20(6): 621-630.

53. Castermans, K., Griffioen, A. W., Tumor blood vessels, a difficult hurdle for infiltrating leukocytes. (2007) Biochim Biophys Acta Rev Cancer 1776(2): 160-174.

54. Molema, G. Tumor vasculature directed drug targeting: applying new technologies and knowledge to the development of clinically relevant therapies. (2002) Pharm Res 19(9): 1251-1258.

55. Griffioen, A. W., Tromp, S. C., Hillen, H. F. P. Angiogenesis modulates the tumour immune response. (2002) Int J Expert Pathol 79(6): 363-368.

56. Griffioen, A. W. Anti-angiogenesis: making the tumor vulnerable to the immune system. (2008) Cancer Immunol Immunother 57(10): 1553-1558.